0013-4651/2003/150(10)/C740/5/$7.00 © The Electrochemical Society, Inc.

Characteristics of Tungsten Carbide Films Prepared by Plasma-Assisted ALD Using Bis(tert-butylimido)bis(dimethylamido)tungsten

Do-Heyoung Kim,[a,c,*,z] Young Jae Kim,[a] Yo Soon Song,[a] Byung-Teak Lee,[b] Jin Hyeok Kim,[b] Seigi Suh,[c] and Roy Gordon[c,*]

[a]*Faculty of Applied Chemical Engineering and Research Institute for Catalysis and* [b]*Department of Materials Science and Engineering, Photonic and Electronic Thin Film Laboratory, Chonnam National University, KwangJu 500-757, Korea*
[c]*Department of Chemistry and Chemical Biology, Harvard University, Cambridge, Massachusetts 02138, USA*

Tungsten carbide (WC_x) thin films were prepared by plasma-assisted atomic layer deposition (ALD) using bis(tert-butylimido)bis(dimethylamido)tungsten at 250°C. The effects of plasma pulse time, radio frequency power, and the N_2/H_2 ratio on the film properties, such as resistivity, surface roughness, step coverage, and stability in air, were examined. The film growth rate (thickness/cycle) was in the range 0.04-0.07 nm/cycle and the resistivity of the films varied from 295 to 22,000 $\mu\Omega$ cm, depending on the plasma conditions. The films were smooth and the conformality of the films deposited in 0.15 μm holes with an aspect ratio of 15:1 was 100%.
© 2003 The Electrochemical Society. [DOI: 10.1149/1.1610000] All rights reserved.

Manuscript submitted November 19, 2002; revised manuscript received April 29, 2003. Available electronically September 2, 2003.

The technical demands of faster and smaller integrated circuit (IC) devices have led to a drive to replace aluminum (Al) and Al alloys used in interconnects with copper (Cu).[1-2] However, Cu diffuses into silicon (Si) and silicon dioxide (SiO_2) readily and thus a stable barrier against diffusion of Cu is essential to avoid failure of the devices.

Various deposition techniques, physical vapor deposition (PVD) and chemical vapor deposition (CVD), are available for the formation of Cu barrier materials.[3] In spite of the advantage of easy controlability of film composition with PVD techniques, deposition of the conformal films needed for diffusion barriers is becoming extremely difficult using PVD techniques due to their inherent line-of-sight nature.[3] As a possible replacement for PVD techniques, CVD processes have been investigated for the formation of the diffusion barrier because of their better conformality in high-aspect-ratio vias.[4] Unfortunately, traditional CVD does not always yield the conformality required for the fabrication of advanced IC devices.[5] Therefore, a specially modified CVD, called atomic layer deposition (ALD), also known as alternating layer deposition or atomic layer epitaxy (ALE), has recently received great attention as a promising deposition technique for the barriers.[6-8] Due to the self-limited reaction nature on the surface of ALD processes, it is possible to control film thickness very accurately and also achieve excellent film uniformity and conformality over large areas. In addition, ALD allows lower deposition temperatures compared to those used in CVD due to more reactive precursors being used because potential side reactions in the gas phase are prevented in ALD.[9]

Tungsten carbides (WC_x), nitrides (WN_x), and tungsten carbonitrides (WC_xN_y) have been demonstrated to be suitable barrier materials against copper diffusion.[10-19] However, in the literature there are no reports on WC_x ALD, in spite of a great amount of research interest in WC_x. In this work we report plasma-assisted metallorganic ALD (MOALD) of WC_x for the first time using a new precursor, bis(tert-butylimido)bis(dimethylamido)tungsten (TBIDMW), and the effects of plasma variables on the film properties.

Experimental

WC_x films were prepared on Si substrates covered by SiO_2 (300 nm) in a vertical flow reactor using TBIDMW as a precursor, which is a yellow air-sensitive liquid at room temperature. The films were deposited at temperatures of 225-325°C. The precursor was introduced to the reactor from a container held at 30 ± 1°C by bubbling helium (He) at a flow rate of 140 sccm. One deposition cycle consisted of exposure to the precursor, argon (Ar) purge, plasma exposure, and another Ar purge. Throughout this work, the pulse length of TBIDMW and the following Ar purge (300 sccm) time were fixed at 5 and 35 s, respectively. A capacitive coupled radio frequency (RF) plasma (13.56 MHz) generator was used to produce 50-250 W power, plasma duration time was varied from 10 to 60 s, and plasma gas composition was either 100% H_2, 50% H_2/50% N_2, or 100% N_2. The impurity levels in the films were estimated using Auger electron spectroscopy (AES) and resistivities were determined from the product of the sheet resistance measured using a four-point probe and the film thickness. The thicknesses of the samples were determined using X-ray reflection (XRR). Because the resistivity of metallorganic-based nitrides is known to increase upon air exposure, the sheet resistance of the films was measured within 5 min of unloading the samples from the reactor.[16,17] Surface roughness, morphology, step coverage, and crystallinity were analyzed using atomic force spectroscopy (AFM), scanning electron microscopy (SEM), and X-ray diffraction (XRD).

Results

Film growth rate.—The effects of plasma pulse time, power, and the N_2/H_2 ratio on the growth rate of WC_x films were investigated at 250°C. The cycle for the precursor pulse and plasma exposure was set to 5 and 10 s, and purging time between the pulses was 35 s. Using identical conditions to the plasma reaction but replacing the hydrogen plasma with ammonia gas (NH_3), no appreciable film growth rate was seen below 300°C. The temperature of 250°C was selected to ensure the absence of any significant decomposition of the precursor, based on the experimental results on film growth rate *vs.* deposition temperature as shown in Fig. 1. The growth rate is almost independent of growth temperature in the range 200-300°C. In addition, a 5 s TBIDMW pulse was selected for this work to supply an abundant dose of TBIDMW, although a 4 s precursor pulse was enough to achieve saturation. No marked increase in growth rate was observed with pulse lengths greater than 4 s. The purging time of 35 s after both the precursor pulse and plasma exposure was also sufficient to remove excess reactants and byproducts from the reactor.

A typical feature of ALD processes is the linear relationship of film thickness to the number of cycles. As can be seen in Fig. 2, it was quite linear, suggesting the conditions investigated resulted in

* Electrochemical Society Active Member.
[z] E-mail: kdhh@chonnam.ac.kr

Downloaded 21 Apr 2011 to 128.103.93.241. Redistribution subject to ECS license or copyright; see http://www.ecsdl.org/terms_use.jsp

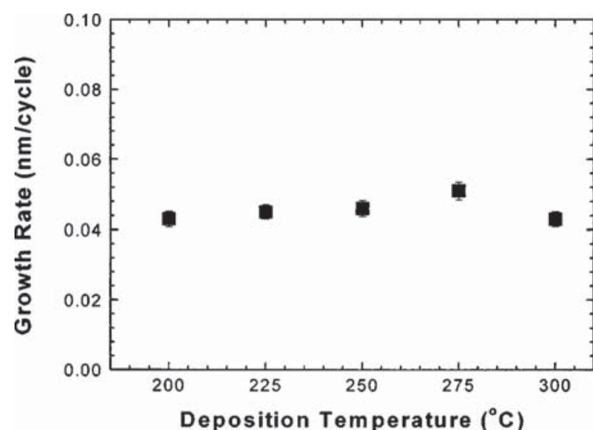

Figure 1. Film thickness as a function of deposition temperature: T_{dep} = 250°C, plasma gas H_2, plasma pulse time 10 s.

ALD-type growth. The film growth rate was estimated to be about 0.046 ± 0.002 nm/cycle.

Figure 3 shows the effect of plasma pulse time on the film growth rate. The plasma exposure time was varied from 10 to 60 s using a 250 W hydrogen plasma. Although saturation of film growth rate was expected at least in a region of short pulse time, extending the length of the plasma pulse resulted in increased film growth rate. The film growth rate was nearly constant with increasing plasma power (Fig. 4).

Figure 5 shows the effect of plasma composition on film growth rate. The percentage of H_2 was set to 0, 50, and 100% at the fixed conditions of 5 s TBIDMW pulse, 10 s plasma pulse, 250 W plasma power, and 35 s Ar purge. The growth rate of the films decreased with increasing H_2 percentage. The growth rate under nitrogen plasma was ~25% higher than that under hydrogen plasma.

Resistivity, film composition, and film stability in air.—Figures 3 and 4 show the effects of plasma exposure time and power on the resistivities of the films. Unlike the film growth rate, a decrease in the resistivity of the films can be clearly seen with increasing plasma pulse time (Fig. 3). The lowest resistivity value was ~295 μΩ cm for an ~14 nm thick film prepared with 60 s plasma pulse. Higher plasma power also yielded films of lower resistivity. As the plasma power was increased from 50 to 200 W, resistivity of the films decreased from 900 to 450 μΩ cm. However, there was no noticeable further decrease with plasma power above 200 W (Fig. 4).

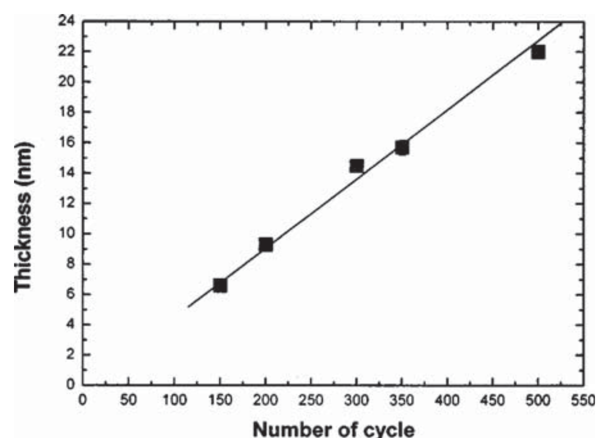

Figure 2. Film thickness as a function of number of cycles.

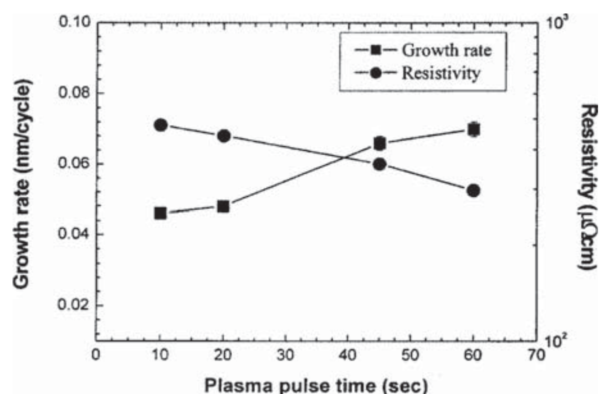

Figure 3. The effect of plasma treatment on film growth rate and resistivity: T_{dep} = 250°C, plasma gas H_2, plasma power 250 W.

Figure 5 shows the effect of plasma gas composition on resistivity. Higher H_2 percentages in the plasma yielded films of much lower resistivity. Although the growth rate differed only within 50% in these experiments, the resistivity of the films ranged over two orders of magnitude, 470 and 22,400 μΩ cm under H_2 and N_2 plasma, respectively.

To investigate the effects of plasma variable on film composition, AES analysis was conducted and the results are summarized in Table I. The concentrations of the tungsten, carbon, nitrogen, and oxygen in the PAALD films were in the range 54-63%, 28-42%, 2-7%, and 1-6%, respectively. The PAALD films are tungsten carbide rather than the tungsten nitride that we expected to result from these depositions, based on results from analogous TaN and TiN experiments.[7,20] The high carbon incorporation seen by compositional AES analysis suggests that use of plasma leads to decomposition of the ligands rather than their displacement. The oxygen in the bulk of the films is believed to originate from air exposure, because the precursor does not contain oxygen in its structure. This diffusion of oxygen into MO-based ALD metal nitride films upon air exposure is well known.[7,21,22]

The results of compositional analysis showed a decrease in carbon content with longer H_2 plasma exposure time. Also, the carbon concentration was reduced from ~42 to ~28% by decreasing the power to 50 from 250 W, along with an increase in nitrogen levels from ~2.5 to 7%. For the case of nitrogen plasma, the films revealed an increase of nitrogen content from ~5 to 6% along with lower carbon levels compared to the films made with a hydrogen

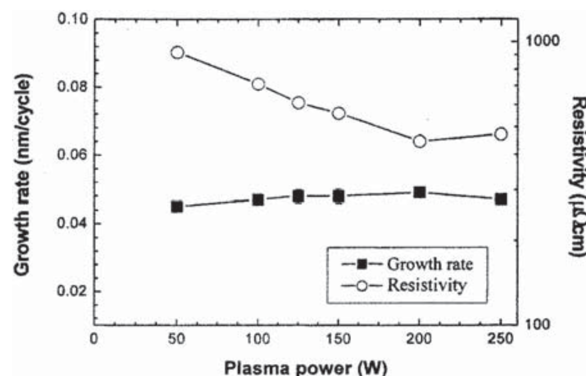

Figure 4. The effect of plasma power on film growth rate and resistivity: T_{dep} = 250°C, plasma gas H_2, plasma pulse time 10 s.

Downloaded 21 Apr 2011 to 128.103.93.241. Redistribution subject to ECS license or copyright; see http://www.ecsdl.org/terms_use.jsp

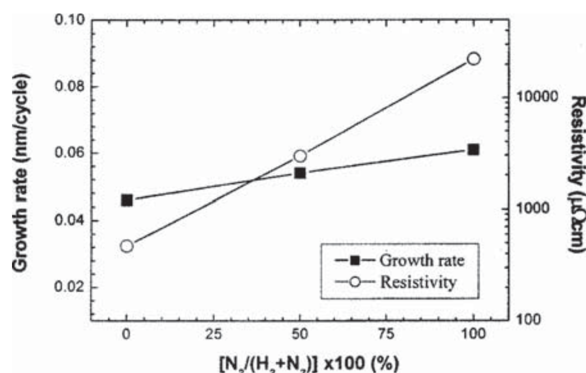

Figure 5. The effect of plasma gas composition on film growth rate and resistivity: $T_{dep} = 250°C$, plasma power 250 W, plasma pulse time 10 s.

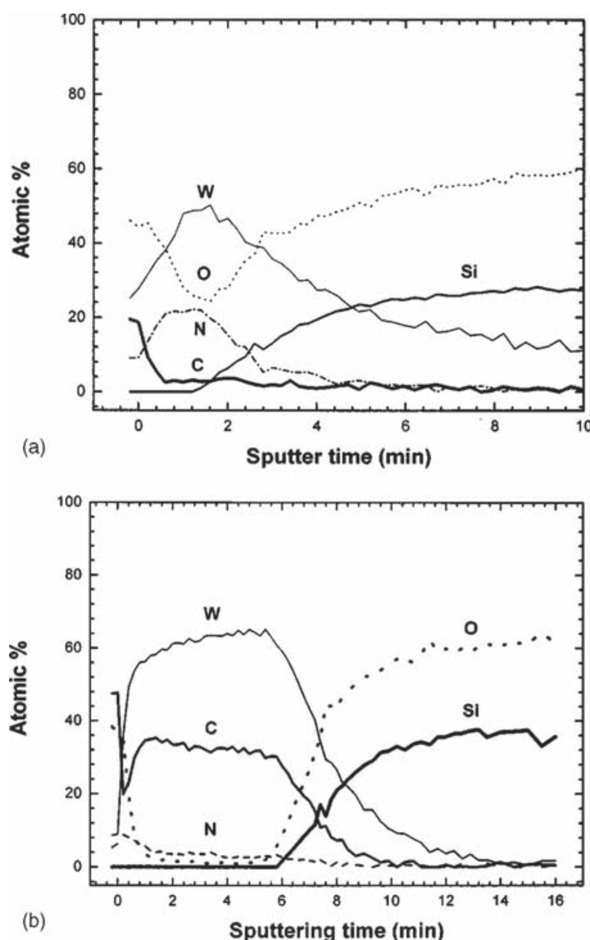

Figure 6. AES depth profile: (a) with NH_3, $T_{dep} = 300°C$; (b) with H_2 plasma, $T_{dep} = 250°C$.

plasma, as well as significant increase in film resistivity, as described earlier.

For comparison, AES analysis was also conducted with the sample deposited at 250°C at the same conditions except replacing the H_2 plasma exposure step with a NH_3 pulse. The thermal ALD film contains a much lower content of carbon, ~3%, compared to those of PAALD films, >~42%, as shown in Fig. 6, indicating a tungsten nitride film. Consequently, the predominant deposition mechanisms for the thermal and plasma TBIDMW-based ALD are different.

Because there are many reports on an aging of the metallorganic-based TiN and TaN in the air, the change of resistivities was evaluated with the WC(N) films deposited by thermal and plasma ALD.[7,21,22] Figure 7 shows the stability of the typical sample in air. The resistivity of the films grown under plasma ALD increases about 2-11% after 24 h in air, and the films deposited at higher power or with longer plasma exposure reveal better stability in air. For example, resistivitiy increased ~11% for the films deposited with 50 W power but only ~3% with 250 W. Also, resistivity increased ~7% for the films deposited with nitrogen but only ~3% with hydrogen as a plasma gas. However, there was a 50% increase in resistivity in the case of thermal ALD films seen after 24 h air exposure. As was shown in Table I, oxygen content in the film was 1-6% for PAALD films and ~27% for thermal ALD films. It is well known that oxygen incorporation in MO-based metal nitride films upon air exposure is due to the low density of deposits. Therefore it is thought that higher density films were prepared by PAALD compared with thermal ALD based on AES analysis and aging analysis of the films.

Crystallinity, surface roughness, and step coverage.—Figure 8 shows the XRD patterns of selected samples deposited under various conditions. Although peak assignments were not possible due to low signal-to-noise ratio, it can be seen that the films grown with relatively high power and longer hydrogen plasma exposure time are more crystalline. However, no peaks were evident in the spectra of the films grown by thermal ALD. Also, unlike the cases using hydrogen plasma, there were no distinct peaks representing a crystal phase in the films deposited using nitrogen plasma. From the compositional and structural analysis it may be deduced that the cause of the significant difference in the resistivities of the films prepared by hydrogen and nitrogen plasmas is caused mainly by structural changes of the films.

AFM was used to evaluate the surface roughness of the films. There were no distinguishable effects of plasma power on surface roughness. The root-mean-square (rms) roughness of the films deposited at 50, 125, and 250 W for 10 s hydrogen plasma exposure was 0.402 ± 0.03, 0.44 ± 0.03, and 0.413 ± 0.03 nm, respectively. This is an interesting result because the roughness did not change with the increase in plasma power, although the crystallinity increased with the power. However, long plasma exposure was seen

Table I. Chemical compositions of the PEALD WC_x films (from AES depth analysis).

Deposition conditions			Composition (atom %)			
Gas	Power (W)	Exposure (s)	Tungsten	Nitrogen	Carbon	Oxygen
H_2 plasma	250	10	54 (±6)	2.5 (±0.5)	42 (±5)	1.5 (±0.5)
H_2 plasma	250	60	63 (±4)	3 (±1)	33 (±3)	1 (±0.5)
H_2 plasma	50	10	59 (±4)	7 (±3)	28 (±1)	6 (±2)
N_2 plasma	250	10	55 (±5)	6 (±1)	36 (±5)	2 (±1)
NH_3 (thermal)	-	10	~58	~22	~3	~27

Downloaded 21 Apr 2011 to 128.103.93.241. Redistribution subject to ECS license or copyright; see http://www.ecsdl.org/terms_use.jsp

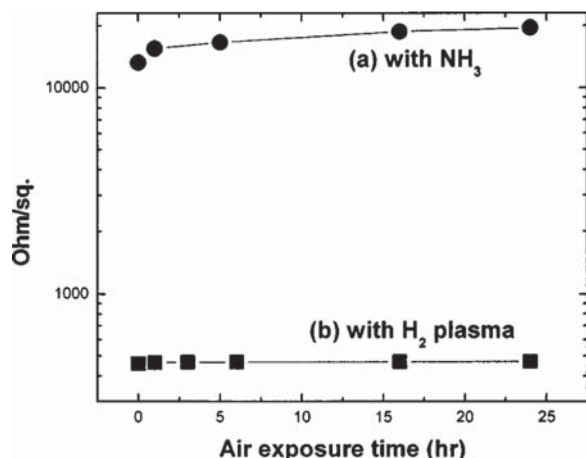

Figure 7. Sheet resistance of the WC films prepared with (a) NH_3 and (b) H_2 plasma as a function of air exposure time.

to roughen the surface. The rms roughness of the films deposited with 30 and 60 s of hydrogen plasma exposure were 0.658 ± 0.03 and 0.828 ± 0.04 nm, respectively. The increased roughness with longer pulse time of hydrogen plasma may be attributed in part to increased crystallinity, as shown in Fig. 8. Use of nitrogen as a plasma gas also results in a rougher surface, 0.51 ± 0.03 nm, but using ammonia as a reducing agent results in a smooth surface, 0.357 ± 0.02 nm.

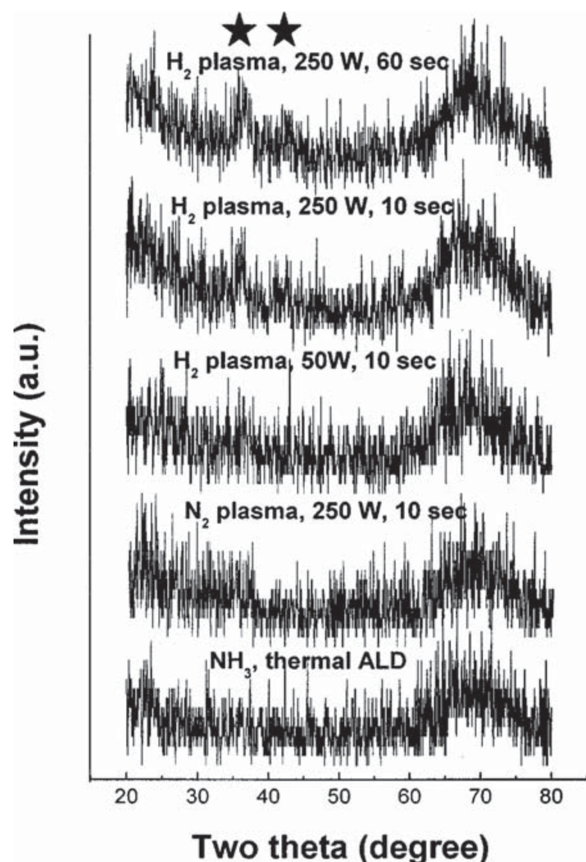

Figure 8. XRD patterns of the WC_x films deposited at various conditions.

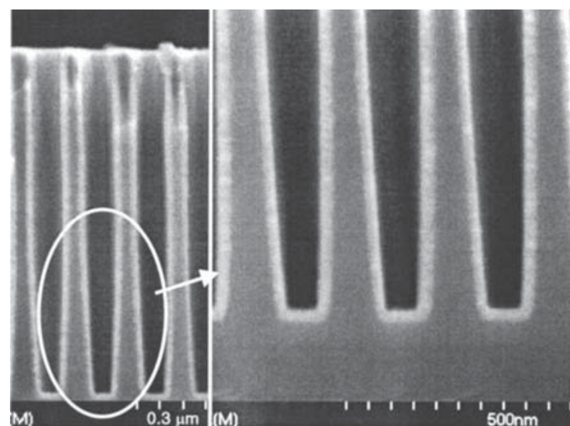

Figure 9. A cross-sectional SEM micrograph of 22 nm thick WC_x film grown using H_2 plasma of 250 W for 10 s exposure at 250°C.

Step coverage was examined by SEM with a sample of 22 nm thick WC_x film deposited on contact holes of 0.15 μm with an aspect ratio of 15:1. As shown in Fig. 9, the PEALD film shows excellent step coverage. There were no measurable thickness variations between the bottom, sidewalls of the holes, and the field surface of the substrate. The excellent step coverage of the WC_x films is evidence that the experiments reported in this work indeed belong to the ALD regime.

Discussion

The linearity of the film thickness *vs.* number of cycles and ~100% step coverage support the belief that the conditions investigated in this work are in the ALD mode, as intended (Fig. 2 and 9). The roles of the plasma in a deposition system can be categorized into three modes, physical, chemical, and physicochemical. Although these three modes of the role of plasma generally occur simultaneously in the PAALD system, one or two modes predominantly act in the formation of the films depending on the process conditions. In the case of an inert gas-based plasma system, physical effects are overwhelming in a PAALD process, because the radicals of the nonreactive gases would not have any chemical reactivity with adsorbed precursors on the surface of the substrates. Consequently, the use of inert gases for plasma results in sputtering, implantation, and densification of the films formed already as well as cracking the adsorbed precursor through bombardment of the radicals. In addition to these physical effects, effects of chemical and physicochemical nature are seen when using reactive gases (for example, hydrogen) as plasma gases, as in this work. Here, chemical role means direct chemical reactions between the activated species with the adsorbed precursors to form films. The physicochemical role represents the conversion of hydrocarbons in the films into volatile C-H compounds. The activated hydrogen in the plasma plays a role as not only a reactant for the formation of the films, but also in removing C-H species in the films already formed in the previous cycle. The incorporation of hydrocarbons in many nitrides prepared using MO precursors is well known.[7,23]

Figures 3 and 4 show the effect of pulse time and power of hydrogen plasma on the film growth rates. The growth rate was observed to slightly increase with increasing plasma exposure time, while no significant changes were seen with increasing plasma power. As described before, if the physical and/or physicochemical roles of the hydrogen plasma are dominant, the growth rate decreases with either increasing plasma pulse time or increasing

Downloaded 21 Apr 2011 to 128.103.93.241. Redistribution subject to ECS license or copyright; see http://www.ecsdl.org/terms_use.jsp

plasma power. For example, Park *et al.* recently reported results on a PAALD TaN_x system of tertbutylimidotris-(diethylamido)-tantalum (TBTDET) using hydrogen plasma.[7] TBTDET is structurally and chemically very similar to TBIDMW, which was used for the WC_x films in this work. With increasing plasma pulse length, they observed an increase in the growth rate of TaN_x up to a 10 s plasma pulse, then a decrease of the growth rate with higher plasma exposure times. They observed no change in film composition with increasing plasma pulse time, only increased density. This may indicate that the reactions to form TaN_x in their system are quickly terminated, and thus the hydrogen plasma does not act as a chemical reactant after 10 s.

In contrast, we observed a compositional change of the WC_x films with varying plasma pulse time. This change of film composition suggests that the effect of physical bombardment of the hydrogen plasma on the PAALD WC_x growth process here is not as great as in the case of TBTDET-based TaN_x PAALD system.

From the results of this work and that of Park *et al.*, it may be seen that the reaction rate of WC_x formation is slow relative to TaN_x under the conditions investigated. This results in the increase in film growth rate with increasing plasma exposure time that we observed. We postulate that the chemical effect is more important than physical and physicochemical effects in the hydrogen-plasma-based WC_x PAALD process.

Increase of carbon concentration in the WC_x films resulted from increasing plasma power. One may presume that the physical bombardment leads to greater carbon incorporation. However, there seem to be other reasons for this phenomenon, because no significant change in the growth rate was observed with increasing plasma power. If high power helps to form WC_x more effectively, then the growth rate should increase. In addition, higher carbon levels in the films deposited with hydrogen plasma are observed relative to those deposited with nitrogen plasma, while use of nitrogen plasma gives an increase in the growth rate. Increased incorporation of nitrogen may partially contribute to the observed higher growth rate with nitrogen plasma. However, causes of high carbon content with the hydrogen plasma films are not well understood. If the films were formed through simple fragmentation of the precursor via bombardment of the activated species, more carbon content in the deposits with nitrogen plasma would be seen, because the mass of the nitrogen is greater than hydrogen, leading to more effective "cracking" of the precursor. Therefore, it is thought that the increased carbon content with increasing plasma power is not only due to the physical effect but also a chemical effect, *i.e.*, the roles of hydrogen radicals are different from those of the nitrogen radicals and there are unknown chemical activities of the hydrogen plasma in the TBIDMW-based PAALD system.

Increasing pulse time and hydrogen plasma power resulted in lower resistivity of the WC_x films. However, as can be seen in Table I, there was no direct relationship between the carbon levels and resistivity. At the same time, the films grown with longer exposure time and higher hydrogen plasma power revealed greater crystallinity, as shown in Fig. 8. Therefore, it may be conjectured that the importance of the crystallinity of the films to resistivity is relatively greater than that of the carbon levels. It is also noteworthy that the resistivity of the films prepared with nitrogen plasma is much higher than that of the films made with hydrogen plasma, in spite of small difference in carbon content ($\sim$38 and 42% of carbon for the films with nitrogen plasma and hydrogen plasma). The higher resistivity of the films deposited using nitrogen plasma may be attributed in part to the less crystalline nature.

Based on these observations, although it is thought that chemical effects are more dominant than the physical effects in TBIDMW-based PAALD system, further analytical studies on reaction mechanisms, bonding status, and microstructures will be needed for a clear understanding of the roles of the radicals and also the relative contributions of chemical, physical, and physicochemical modes in WC_x PAALD systems.

Conclusions

We have explored PAALD using TBIDMW with hydrogen and nitrogen plasmas under various plasma exposure times and rf power. Use of the plasma leads to the formation of tungsten carbide films, but tungsten nitride films are obtained from thermal ALD with ammonia. This indicates that hydrogen radicals act as a aid to precursor decomposition rather than as a reducing agent of the alkyl groups in the precursor. Although the films deposited using hydrogen plasma contain significant amounts of carbon, the films have resistivities four times lower than those of the films deposited using ammonia only.[19] Also, the PAALD films had excellent stability in air. The use of nitrogen in the plasma helped to improve the film's stability but also resulted in an increase in resistivity. Higher power and longer exposure time of the hydrogen plasma was effective in increasing the crystallinity of the films, decreasing film resistivities.

The surface topography of the films was very smooth, but longer plasma pulse times tended to roughen the surface of the deposits. Resistivities as low as 295 $\mu\Omega$ cm and perfectly conformal films on contact holes with an aspect ratio of 15:1 were obtained.

Acknowledgment

This work was supported by Korea Ministry of Science and Technology through the National Research Laboratory program. D.H. Kim would like to thank Jeffrey Barton for useful help.

Chonnam National University assisted in meeting the publication costs of this article.

References

1. International Technology Roadmap for Semiconductors, http://public.itrs.net/Files/2001ITRS
2. S. P. Murarka, *Mater. Sci. Eng., R.,* **19**, 87 (1997).
3. S.-Q. Wang, *MRS Bull.,* **19**, 30 (1994).
4. A. Jain, O. Adetutu, B. Ekstrom, G. Hamilton, M. Herrick, R. Venkatraman, and E. Weitzman, *Mater. Res. Soc. Symp. Proc.,* **564**, 269 (1999).
5. D. H. Kim, G. T. Lim, S. K. Kim, J. W. Park, and J. G. Lee, *J. Vac. Sci. Technol. B,* **17**, 2197 (1999).
6. M. Juppo, P. Alen, M. Ritala, T. Sajavaara, J. Keinonen, and M. Leskela, *Electrochem. Solid-State Lett.,* **5**, C4 (2002).
7. J. S. Park, H. S. Park, and S. W. Kang, *J. Electrochem. Soc.,* **148**, C28 (2002).
8. H. Jeon, J. W. Lee, Y. D. Kim, D. S. Kim, and K. S. Yi, *J. Vac. Sci. Technol. A,* **18**, 1595 (2000).
9. M. Ritala and M. Leskela, *J. Phys. IV,* **9**, Pr8-837 (1999).
10. Y. M. Sun, S. Y. Lee, A. M. Lemonds, E. R. Engbrecht, S. Veldman, J. Lozano, J. M. White, J. G. Ekerdt, I. Emesh, and K. Pfeifer, *Thin Solid Films,* **397**, 109 (2001).
11. S. J. Wang, H. Y. Tsai, S. C. Sun, and M. H. Shiao, *J. Electrochem. Soc.,* **148**, G500 (2001).
12. H. Li, S. Jin, H. Bender, F. Lanckmans, L. Heyvaert, K. Maex, and L. Froyen, *J. Vac. Sci. Technol. B,* **18**, 242 (2000).
13. B. L. Park, D. H. Ko, Y. S. Kim, J. M. Ha, Y. W. Park, S. I. Lee, H. D. Lee, M. B. Lee, U. I. Chung, Y. B. Koh, and M. Y. Lee, *J. Electron. Mater.,* **26**, L1 (1997).
14. C.-W. Lee, Y. T. Kim, and J. Y. Lee, *Appl. Phys. Lett.,* **64**, 619 (1994).
15. S. Smith, W. M. Li, K. E. Elers, and K. Pfeifer, *Microelectron. Eng.,* **64**, 247, (2002).
16. J. W. Klaus, S. F. Ferro, and S. M. George, *J. Electrochem. Soc.,* **147**, 1175 (2000).
17. J. W. Klaus, S. F. Ferro, and S. M. George, *Appl. Surf. Sci.,* **162-163**, 479 (2000).
18. K. E. Elers, V. Saanila, P. J. Soininen, W. M. Li, J. T. Kostamo, S. Haukka, J. Juhanoja, and W. F. A. Besling, *Chem. Vap. Deposition,* **8**, 149 (2002).
19. J. Becker, S. Suh, and R. G. Gordon, Unpublished data.
20. D. H. Kim, Unpublished data.
21. D. H. Kim, J. J. Kim, J. W. Park, and J. J. Kim, *J. Electrochem. Soc.,* **143**, L188 (1996).
22. A. Intermann, H. Koerner, and F. Koch, *J. Electrochem. Soc.,* **140**, 3215 (1993).
23. J. H. Yun, E. S. Choi, C. M. Jang, and C. S. Lee, *Jpn. J. Appl. Phys., Part 2,* **41**, L418 (2002).

Downloaded 21 Apr 2011 to 128.103.93.241. Redistribution subject to ECS license or copyright; see http://www.ecsdl.org/terms_use.jsp